AD-A257 551

OFFICE OF NAVAL RESEARCH

Technical Report No. 10

Pulsed Laser Deposition of
Amorphous Diamond-like Carbon
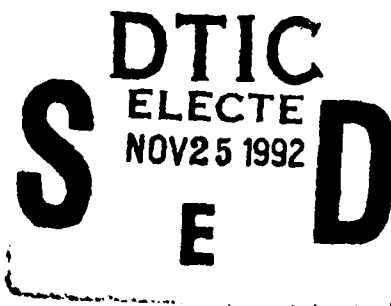Films With ArF (193 nm) Excimer Laser

by

F. Xiong, Y.Y. Wang, V. Leppert, R.P.H. Chang

prepared for publication in the

Journal of Materials Research

Northwestern University
Dept. of Materials Science and Engineering,
Evanston, IL 60208

DTIC
S ELECTE
NOV25 1992
E D

November 1992

92-30212

REPORT DOCUMENTATION PAGE

1. AGENCY USE ONLY (Leave blank)	2. REPORT DATE Nov. 1992	3. REPORT TYPE AND DATES COVERED Technical

4. TITLE AND SUBTITLE

Pulsed laser deposition of amorphous diamond-like carbon films with ArF (193 nm) excimer laser

5. FUNDING NUMBERS

G N0001489J1848
R&T code 413u002

6. AUTHOR(S)

F. Xiong, Y.Y. Wang V. Leppert, R.P.H. Chang

7. PERFORMING ORGANIZATION NAME(S) AND ADDRESS(ES)

Materials Science & Engineering Dept.
Northwestern University
2225 Sheridan Road
Evanston, IL 60208

8. PERFORMING ORGANIZATION REPORT NUMBER

Technical Report # 10

9. SPONSORING/MONITORING AGENCY NAME(S) AND ADDRESS(ES)

Chemistry Division
Office of Naval Research
800 N. Quincy Street
Arlington, VA 22217-5000

10. SPONSORING/MONITORING AGENCY REPORT NUMBER

11. SUPPLEMENTARY NOTES

12a. DISTRIBUTION/AVAILABILITY STATEMENT

This document has been approved for public release and sale; its distribution is unlimited.

12b. DISTRIBUTION CODE

13. ABSTRACT (Maximum 200 words)

We have deposited hydrogen-free diamond-like amorphous carbon (amorphous diamond) films by ArF (193 nm) pulsed laser ablation of graphite. The deposition process is performed with the laser power density of only 5×10^8 W/cm^2 at room temperature without any auxiliary energy source incorporation. The resulting films possess remarkable physical, optical and mechanical properties which are close to those of diamond and distinct from the graphite target used. The films have a mechanical hardness up to 38 GPa, an optical energy band gap of 2.6 eV and excellent thermal stability. Analysis of electron energy loss spectroscopy reveals the domination of diamond-type tetrahedral bonding structure in the films with the sp^3 bond fraction over 95%. Compared to other reported results of pulsed laser deposited diamond-like carbon films, our experimental results confirm that the laser wavelength or photon energy plays a crucial role in controlling the properties of the pulsed laser deposited diamond-like carbon films.

14. SUBJECT TERMS

Diamond-like carbon films

15. NUMBER OF PAGES
30

16. PRICE CODE

17. SECURITY CLASSIFICATION OF REPORT	18. SECURITY CLASSIFICATION OF THIS PAGE	19. SECURITY CLASSIFICATION OF ABSTRACT	20. LIMITATION OF ABSTRACT
Unclassified	Unclassified	Unclassified	UL

PULSED LASER DEPOSITION OF AMORPHOUS DIAMOND-LIKE CARBON FILMS WITH ArF (193 nm) EXCIMER LASER

Fulin Xiong, Y. Y. Wang, V. Leppert, and R. P. H. Chang

Department of Materials Science and Engineering and Materials Research Center, Northwestern University, 2225 Sheridan Road, Evanston, IL 60208

ABSTRACT

We have deposited hydrogen-free diamond-like amorphous carbon (amorphous diamond) films by ArF (193 nm) pulsed laser ablation of graphite. The deposition process is performed with the laser power density of only 5×10^8 W/cm^2 at room temperature without any auxiliary energy source incorporation. The resulting films possess remarkable physical, optical and mechanical properties which are close to those of diamond and distinct from the graphite target used. The films have a mechanical hardness up to 38 GPa, an optical energy band gap of 2.6 eV and excellent thermal stability. Analysis of electron energy loss spectroscopy reveals the domination of diamond-type tetrahedral bonding structure in the films with the sp^3 bond fraction over 95%. Compared to other reported results of pulsed laser deposited diamond-like carbon films, our experimental results confirm that the laser wavelength or photon energy plays a crucial role in controlling the properties of the pulsed laser deposited diamond-like carbon films.

DTIC QUALITY I

Accesion For		
NTIS CRA&I		☒
DTIC TAB		☐
Unannounced		☐
Justification		
By		
Distribution /		
Availability Codes		
Dist	Avail and / or Special	
A-1		

1

I. INTRODUCTION

While much effort has been spent on growing diamond through the metastable synthesis processes at low temperatures and low pressures, deposition of amorphous diamond-like carbon (DLC) films has also been attracting a great deal of attention.[1-3] Even though the terminology of DLC is rather imprecise, DLC films may include many amorphous forms of carbon with or without hydrogen. They have many properties close or similar to those of diamond and are distinct from those of graphite. In particular, the smooth surface morphology and homogeneity of DLC films make them more useful than polycrystalline diamond films in many applications.[2-3] Among the various methods for preparing DLC films, such as ion beam deposition, sputtering, plasma assisted chemical vapor deposition, and cathodic arc, pulsed laser deposition has been shown to be one of the most attractive techniques.[3-10] It can produce films without hydrogen and with high degree of diamond-like properties. Hence, films of this kind have been given the name amorphous (or amorphic) diamond in the literature.[4,10]

Several types of lasers have been used for the deposition of DLC films, including KrF (248 nm) and XeCl (308 nm) pulsed excimer lasers,[4-7] Nd:YAG (1064 and 532 nm) lasers,[8-10] and pulsed ruby laser (683 nm) laser[11] as well as CO_2 CW laser.[12] The wavelength ranges from the ultraviolet to the infrared, and the power density from 10^8 W/cm^2 to 10^{11} W/cm^2. In general, the degree of diamond-like character (mainly the fraction of sp^3 hybridized carbon bonding in a film) varies considerably with the deposition parameters. Commonly, it is believed that pulsed laser deposition is an energetic process.[13] The laser power density plays a vital role in controlling the film properties. There is a threshold at 10^{11} W/cm^2 in order to grow high quality DLC films.[8-10] In this paper we report the results of pulsed laser deposition of DLC films using an ArF excimer laser (193 nm, the shortest wavelength used so far for DLC film deposition). The structural, optical, electronic, and physical properties of the films have been investigated. Excellent diamond-like properties of the films have been obtained with the laser power density only in the range of 5x10^8 W/cm^2 without any auxiliary energy source. This result has convinced us that the laser photon energy is a key factor in the control of the diamond-like properties of the pulsed laser deposited DLC films.

2

II. EXPERIMENTAL

The experimental apparatus of the pulsed laser ablation system for film deposition is very simple, schematically shown in Figure 1. It consists of a stainless steel high vacuum chamber pumped by a turbo-molecular pump with a base pressure of 1×10^{-7} Torr. An ArF pulsed laser beam (Questek Model 2470SC) with the wavelength of 193 nm and the pulse duration of 21 ns (FWHM) is introduced into the chamber through an anti-reflection coated convex focus lens and a supersil quartz window. The stabilized output energy of 300 mJ/pulse and a repetition rate of 5 or 10 Hz are normally used. The laser beam impacts the target at an angle of 45° to the surface normal and has a spot size of 1x2 mm² at the target surface. After considering the power loss through the air path and the chamber window, the instantaneous power density at the target is estimated to be about 5×10^8 W/cm². A 1 inch diameter pyrolytic graphite (PG) disk is used as an ablation target. It is kept rotating at 10 RPM during the process. The laser plume is emitted along the surface normal of the target, intensified within a few millimeters near the surface in a bluish-white color, then expanding forward in a reddish cone. The unheated substrate is placed about one inch away and parallel to the target. A typical deposition rate of 0.1 nm/pulse is obtained, slightly varying with the deposition conditions, such as the vacuum condition and laser pulse energy.

N-type Si(100) wafers (resistivity 0.1 Ω-cm), fused quartz slides, and cover glass slides are routinely used as substrates. They are cleaned through a standard degreasing process and finally dipped in HF before loading into the chamber. Freshly cleaved NaCl crystals are utilized with the films for EELS analysis. KBr crystal disks are used for FTIR analysis. Other substrates such as Lexan plastic, stainless steel, Mo and W metal sheets are also tried for potential application.

A variety of analytical techniques have been used for property analysis and structure characterization. These include microhardness measurements with nanoindentation, chemical inertness tests in acid solutions, optical transmission tests in the region from near IR to UV, and electrical conductivity test with a simple surface-to-back Ohmic probe. Several spectroscopic methods, such as electron microscopy (SEM

3

and TEM), electron energy loss spectroscopy (EELS), Raman spectroscopy, Fourier transform infrared spectroscopy (FTIR) as well as spectroscopic ellipsometry have been used to characterize the films. High energy ion elastic forward scattering spectroscopy is used for detection of hydrogen content in the films. The technical details of all these characterization will be described in the next section.

III. FILM CHARACTERIZATION AND RESULTS

1. General

Generally, the films deposited on Si wafers or glass slides were mirror-like smooth. They normally appeared golden brownish at the center with colorful thickness interference patterns at the edge. At present, no efforts have been made to improve thickness uniformity. SEM examination revealed the surface morphology to be extremely smooth. The plan-view TEM and selected area diffraction (SAD) indicated that both films were homogenous and in an amorphous phase. Two diffused ordinary amorphous rings were observed in SAD patterns. We have noticed that a cleaner surface and a better vacuum condition can greatly improve the interface adhesion, resulting in a larger thickness limit. We have been able to deposit 1 um thick films without cracking.

Both films passed the chemical inertness test by immersing the films along with the substrate in various acids and organic solutions. The electrical resistivity was simply tested by placing an Ohmic probe on the film surface and the back of the substrate. On the samples with a size of 1x1 cm^2, typical resistance in the 100 MΩ range was obtained.

2. Hydrogen Content

High energy ion elastic forward scattering spectroscopy with 2.0 MeV He$^+$ was performed to determine hydrogen concentration in the films.[14] A spectrum shown in Figure 2 was taken from a sample of a 300 nm DLC film on Si(100). It indicated that the hydrogen content in the film was below the detection limit (less than 0.1%). Only a surface peak of hydrocarbon contamination was shown. Quantitative determination of the hydrogen concentration was made by comparing with a hydrogen-ion-implanted sample (H$_2^+$, 25 keV, 1x10^{17} ions/cm^2). The implanted hydrogen has a Gaussian

4

distribution centered at an estimated depth of 370 nm. This spectrum is also shown in Figure 2 for comparison.

3. Mechanical Hardness

Microhardness measurements were carried out on a Nanoindenter II at Nano Instruments, Inc. Each indentation consisted of loading the diamond indenter tip on the sample surface until a desired penetration depth was obtained, removing 80% of the load and repeating this cycle twice. The hardness and modulus of the film were then determined at each penetration level based on the geometrical dimension of the indentations. Ten indentations were made on each sample. An uncoated Si(100) crystal was measured as a control reference, and the result matches the standard value. The directly recorded results of a film (160 nm thick) on Si(100) are plotted in Figure 3. The film had a hardness between 30-38 GPa and Young's modulus value of about 220~230 GPa. The measured hardness value dropped at a deep penetration where the substrate effect eventually becomes significant. This is consistent with elastic modulus declining to 190 GPa.

4. Optical Properties

Optical properties of the films were examined by spectroscopic ellipsometry analysis. This was performed on a rotating analyzing ellipsometry system (SOPRA, Inc) for the films deposited on Si(100). It automatically measures Tan(psi) and Cos(delta) as a function of the wavelength using the Hadamard transform of the photodetector signals. Spectroscopic scanning covers a range from 1.5 to 5 eV. A microspot of a size of 150x100 μm^2 and an incident angle of 75 degrees from the sample surface normal were used. The optical properties of the films, the real (n) and imaginary (k) components of the complex refractive index, were obtained by fitting the experimental curves with the Cauchy model. Figure 4 shows the n-k values for the sample deposited with 1500 pulses. The n values for diamond[15] and graphite[16] are also plotted for comparison The thickness of the film as determined by spectroscopic ellipsometry was 1450 nm, consistent with the estimated thickness from summing up the total laser pulses. The result was also confirmed by profilometer measurements. The real part of the index of reflection (n), had values in

5

the range of 2.6 to 2.8, higher than diamond and graphite, indicating the dense structure. The trend of the n value was similar to SiC and SiO films, slightly decreasing with the photon wavelength. The optical band gap,[17-18] Eg, was determined by extrapolating the plot of photon energy, E, versus the quantity $E\varepsilon_i^{1/2}$, where $\varepsilon_i=2nk$, the imaginary part of the dielectric function determined by ellipsometry analysis. This is based on the relation $\varepsilon_i(E)=B(E-Eg)^2/E^2$, where B is a constant. A plot for the sample shown in Figure 4 is presented in Figure 5. The band gap energies were found to be 2.6 eV for this film. This is the highest value found so far for the carbon films prepared by the pulsed laser deposition. The extrapolated value of 1.8 eV at the tail part for this film marks a subband gap, which may be due to diffused scattering and impurity absorption.

The optical transmission of a film, which was deposited on fused quartz slides with a thickness of about 100 nm, was also performed from the UV to near IR (the spectrum is not shown). The film had a transmittance of 85% in the near IR and 60% in the visible region.

5. Bonding Structures

The bonding structures of the films have been examined with electron energy loss spectroscopy (EELS). This is carried out on Hitach H-2000 field-emission analytical TEM, operated at an accelerating voltage of 100 keV. The TEM system is equipped with a Gatan electron energy loss spectrometer which has a maximum resolution of 0.5 eV as defined by the FWHM of the zero-loss peak. Two regions of EELS spectra are collected, the low-loss or valence excitation loss spectra (0-50 eV) and the high-loss or carbon K-edge core-loss spectra (250-400 eV). The films deposited on Si(100) and NaCl crystalline substrates have been analyzed. In order to assess the spectra of the pulsed laser deposited films, the spectra of three other forms of carbon have also been acquired under identical conditions. These materials include a polycrystalline diamond film prepared by microwave plasma assisted chemical vapor deposition (CVD), a pyrolytic graphite which was used as the ablation target, and an amorphous carbon film by thermal evaporation. The spectra of the low loss region are shown in Figure 6a. They are taken in an off-angle diffraction at 0.10 A^{-1} in order to avoid complication of the

6

contribution of the surface plasmon, Cerenkov radiation, and energy dependent factor in the formula. The spectrum of graphite has a plasmon peak at 26 eV corresponding to the $\sigma+\pi$ transitions and a large peak at 6.7 eV corresponding to the π to π^* antibonding transitions and representing the sp^2 bonding structure in the sample. The spectrum of the amorphous carbon film shows a very similar characteristic, but the energies of the peaks are slightly lower (24 eV an 6.0 eV) indicating a lower atomic density. The intensity of π^* bond peak at 6.0 eV is very weak, implying its disordered structure and a low fraction of sp^2 bonding. The spectrum of polycrystalline CVD-diamond is different, consisting of a broad peak centered at 33 eV with a prominent shoulder at 24 eV, matching the spectra of natural or synthetic diamond crystals. The spectra of two DLC samples are distinct from that of graphite, consisting of a single broad plasmon peak centered at 29.5 eV for the film on Si(100) and 30 eV for the film on NaCl. A complete lack of $\pi-\pi^*$ antibond transition peak is a sign of the disappearance of sp^2 bonding in the films. The shift to lower energies of the plasmon peak from crystalline diamond may be a result of reduction of the density of the films due to their amorphous structure. But the energy is higher than that of graphite, so is the density. The carbon K-edge spectra of all the specimens are shown in Figure 6b after removal of the background. The main features of the graphite spectrum are a peak at 286 eV corresponding to transitions from 1s to the π^* states, followed by a series of peaks due to transition from 1s to the σ^* states. Again, the amorphous carbon film gives a spectrum similar to that of graphite, with a smaller π^* bond peak, consistent with the result of the low loss spectrum. The CVD-diamond gives distinct spectral features with several narrower peaks above 294 eV, representing transitions only from 1s to the σ^* states. One may notice that a very small shoulder exists where the π^* bond should be. This is true, indicating graphitic impurity in this CVD-diamond film. In the DLC films deposited on Si(100) and NaCl crystals, the spectra show the main structure close to that of diamond. The lack of the crystalline structure order results in a broad peak centered at 296 eV, a smearing out of the fine transition structures from 1s to the σ^* states. A high fraction of tetrahedral bonding (sp^3) has eliminated the intensity of the π^* peak, only a very small shoulder shown in the film deposited on Si(100) substrate. Based on the fact that graphite consists of 100% sp^2-bonding and diamond, 100% sp^3-bonding, We can determine the fraction of sp^3 bondings

7

in a DLC film from the ratio of the π^* peak integral of the net counts in its normalized spectrum to that of graphite.[19-20] The estimated values here for both samples are over 95%, indicating that the films are full of diamond-type tetrahedral bonding. Upon these results and hydrogen-free character of the films, we may also name our films "amorphous diamond."

The bonding structure of the films has also been investigated with FTIR and Raman spectroscopy. In FTIR analysis, the samples were made by depositing 100 nm thick films on 1 inch diameter KBr crystalline disks. The spectra were measured using a Mattson FTIR spectrophotometer in the transmission mode and in the wavenumber range of 400 to 4000 cm^{-1}. The line assignment is based on the molecular vibration modes of organic compounds.[21-22] The film prepared in vacuum is almost IR featureless (the spectrum is not shown here) with only a very small peak at 2930 cm^{-1} for sp^3 C-H asymmetrical stretching mode. This may be originated from surface C-H bonds. Note that this spectrum is distinct from those representative of the a-C:H films which contain a great amount of C-H bonds, while there is negligible hydrogen contained in the films obtained by pulsed laser deposition, as detected by ion scattering analysis shown above.

Raman analysis was performed with a system equipped with a CCD detector. An Ar laser with the wavelength of 514 nm and a power of 200 mW was used. In Figure 7, a typical Raman spectrum of the films is shown together with a spectrum from the PG target used. The PG spectrum gives two well-defined sharp characteristic peaks[23-24] at 1580 cm^{-1} (the graphitic line) and 1350 cm^{-1} (the disordering line), respectively. In the DLC film a broad Raman band appears, which is centered at 1550 cm^{-1}, leading to the disappearance of the disordering line. This is similar to the Raman spectrum of amorphous DLC films with no hydrogen prepared by ion beam sputtering of graphite.[3,25] Since the film is optically transparent, the Si second-order Raman peak at 940-980 cm^{-1} has become more pronounced in this sample. Note that the characteristic line 1320 cm^{-1} for diamond is not shown in this spectrum, even though the film has been confirmed by EELS analysis to contain a diamond-type sp^3 bonding of more than 95%. This might be due to its amorphous structure, which would smear out or eliminate the characteristic

line of crystalline diamond. Secondly, this might be due to a very poor Raman scattering efficiency of diamond line, comparing to that of graphite (1:50).[21] Both theoretical and experimental investigations are suggested to be undertaken in order to understand this interesting phenomena.

6. Thermal Stability

Thermal stability is an important factor to be considered in the application of the DLC films. Based on the optical band gap analysis, it was found[26] that in hydrogenated amorphous carbon films, the optical gap decreases from 2.2 eV to 0 eV as the films are annealed at temperatures of up to 600 °C. This indicates the development of graphitic short range order and the loss of the diamond-like character in the films. It is mainly due to hydrogen decomposition and development of graphitic and void components in the films. We have tested the thermal stability of our DLC films in the same way with optical band gap determination through ellipsometry analysis. The samples were prepared in an identical deposition condition with a film thickness of about 150 nm on Si(100) substrates. These samples were then annealed in a vacuum furnace at temperatures of 300, 450, 600 and 800 °C. Figure 8 displays the results of these samples in the form of the Tauc plot as described before. It shows the evolution of the optical gap Eg change as a function of annealing temperature. Overall, they tell us that the films are thermally stable under high temperature annealing. after annealing at temperature of up to 800 °C, the optical gap of the films maintains same as one at RT (2.6 eV), instead of decreasing to 0 eV as in the case of hydrogenated amorphous DLC films. A relative increase of the ε_i value originates from the increase of the n value, implying increase of the film density, possibly by eliminating the porous structure in the films. This is completely distinct from hydrogenated amorphous DLC films.[24]

IV. DISCUSSIONS

Summarizing our experimental results, using an ArF excimer laser, amorphous carbon films with a high degree of diamond character have been obtained by pulsed laser deposition at room temperature from a graphite target. The resultant films are found to be superior with regard to their diamondlike properties, such as mechanical hardness and

9

optical band gap, to those prepared by pulsed laser deposition with other laser sources which have a longer wavelength. Especially, their hydrogen-free characteristics makes the films thermally stable against high temperature annealing. This is distinctly different from hydrogenated DLC films prepared by other deposition methods. Based on their high fraction of sp^3 hybridized diamond-type bonding as well as other diamond-like properties, we may also name these films "amorphous diamond", though the Raman spectroscopic analysis has unlikely supported this statement.

Pulsed laser deposition has been used to prepare a variety of thin films, from high quality high-Tc superconducting films to semiconductor films, as well as many oxide, nitride and hard carbon films.[27-28] The most important advantage of this technique is the near stoichiometric conservation for the compound materials deposited.[27-28] In contrast, carbon films are neither complex nor multicomponent. High quality DLC films deposited by pulsed laser ablation are believed to result from the nonequilibrium features in the process, such as high speed thermal evaporation, high efficient atomic excitation and electronic ionization, and fast quenching. These lead to the formation of deposited films in metastable states with many unique physical properties. It is suggested[8] that as with all methods for producing such films, the fraction and kinetic energy of ionized deposition species generated by laser ablation is a critical parameter in determination of the film properties. It has been suggested[13] that deposition of sp^3-bonded carbon requires the incoming atomic species to have kinetic energies well above those obtained in thermal processes, such as evaporation. These, in turn, rely on the laser wavelength and power density in the pulsed laser deposition process.

For a comparison, Table 1 lists several reported results of pulsed laser deposited amorphous carbon films with different deposition conditions. Earlier, when a long wavelength CW CO_2 laser[12] was used, only soft and graphitic films were obtained. Improvement of diamond-like quality of the films could be achieved by further ion bombardment. When a pulsed ruby laser was used, insulating and optical transparent films were attained.[11] Marquardt and his coworkers[7] first used a pulsed Nd:YAG laser at the 1052 nm wavelength for film deposition. They found that there existed such a

10

power density threshold above which the films were hard and diamond-like. The estimated value of this threshold was 5×10^{10} W/cm^2. Collins and his coworkers[8,9] used a Nd:YAG laser at 532 nm wavelength and claimed to have observed that threshold. But they had also superimposed a high current discharge to the ablation process in order to obtain DLC films (they termed these films "amorphic diamond"). Sato et al.[4] used a XeCl (308 nm) excimer laser at 3×10^8 W/cm^2 and the films were diamond-like, but they were found to contain 20% hydrogen. Krishnaswamy and co-workers[5,6] used the XeCl laser at 5×10^8 W/cm^2 and hard carbon films were obtained by pulsed laser deposition alone. By superimposing the capacitor discharge to the process for deposition, the carbon films on Si(100) substrates had improved optical and mechanical properties. Recently, KrF (248 nm) excimer laser was used and hard films were obtained directly with no auxiliary energy added.[4-5] In our experiment, the ArF (193 nm) excimer laser was utilized and the films with superior hardness and high optical band gap were found. Summarizing all these results convinced us that the laser wavelength or photon energy has been a crucial parameter for controlling high degree of diamond-like properties of pulsed laser deposited carbon films. Changing the laser wavelength from the IR region to the UV region results in a decrease of the laser power density by an order of 2.

It is not surprising that the pulsed laser deposition with short wavelengths (UV) and short pulse widths (in a ns range) yields superior quality films. This has been proven in the deposition of high-Tc superconductor films[29] and cubic BN films[30]. Presumably, it is due to the increase in the optical penetration depth and photoionization of evaporated materials as well as changes in other secondary processes during ablation. These result in more efficient coupling of the optical energy to the target, the enhancement of production of atomic ion species, and increase of the kinetic energy of ablated species for deposition. In contrast, IR radiations of long wavelength have short penetration depth, resulting in a more thermal-like heating of target materials, so as emission of neutral or ionized cluster species. It was reported by Murray and Dempsey[31] that in a photon ablation process of graphite, 248 nm radiation resulted primarily in the ejection of C_3^+ ions normal to the surface with mean kinetic energies on the order of 20 eV. Changing the wavelength to 193 nm resulted in the ejection of atomic C^+, with a mean

11

kinetic energy near 50 eV. Nd:YAG radiation produced more C_n^+ ($1 < n < 25$) cluster species. Pappas and his coworkers[4] have also reported that in the vapor plume generated by 248 nm KrF excimer laser irradiation of graphite target, the kinetic energy of the C_2 molecule increases linearly with laser power density of up to 12 eV in the moderate power density range (3-5 J/cm^2), then decline in the higher flounce. The C_n^+ cluster ions are 5-10 times more energetic and comprise about 10% of the vapor flux. A comparative experiment was done with a KrF beam and a Nd:YAG (532 nm) beam at a similar deposition condition.[32] The result indicated that the quality of the carbon films deposited by the 248 nm irradiation was diamond-like, and superior to those produced by using the Nd:YAG laser.

V. CONCLUSIONS

In conclusion, diamond-like amorphous carbon (or amorphous diamond) films have been deposited simply by ArF pulsed laser ablation of graphite at room temperature with no other energy incorporated. The laser power density used (5×10^8 W/cm^2) is considerably below the claimed threshold. The resultant films are found to be superior in their mechanical hardness and optical properties to those prepared by laser ablation with other laser sources. These films are free of hydrogen and exhibits excellent thermal stability. Pulsed laser deposition of DLC films with ArF excimer laser has proven to be more versatile than other laser sources due to the higher photon energy, which is believed to increase the number of ionized species and their kinetic energy during laser ablation. We confirm that the high photon energy (or the short wavelength) of the laser sources substantially controls the diamond-like properties of the pulsed laser deposited carbon films.

ACKNOWLEDGEMENTS

REFERENCES

1. J. C. Angus and C. C. Hayman, Science **241**, 913 (1988).

2. *Properties and Characterization of Amorphous Carbon Films*, ed. J. J. Pouch and S. A. Alterovitz, <u>Materials Science Forum</u>, Vol. 52 &53 (trans. Tech. Publications, Switzerland, 1990).

3. H. C. Tsai and D. B. Bogy, J. Vac. Sci. Technol. A **5**, 3287 (1987).

4. D. L. Pappas, K. L. Saenger, J. Bruley, W. Krakow, and J. J. Cuomo, preprint (1992).

5. R. T. Demers and D. G. Harris, SPIE Vol. **1146**, 68 (1989).

6. T. Sato, S. Furuno, S. Iguchi, and M. Hanabusa, Appl. Phys. A **45**, 355 (1988).

7. J. Krishnaswamy, A. Rengan, J. Narayan, K. Vedam, and C. J. Mchargue, Appl. Phys. Lett. **54**, 2455 (1989).

8. C. L. Marquardt, R. T. Williams, and D. J. Nagel, Mat. Res. Soc. Symp. Proc. Vol. **38**, 325 (1985).

9. F. Davanloo, E. M. Juengerman, D. R. Jander, T. J. Lee, and C. B. Collins, J. Appl. Phys. **67**, 2081 (1990).

10. C. B. Collins, F. Davanloo, D. R. Jander, T. J. Lee, H. Park, and J. H. You, J. Appl. Phys. **69**, 7862 (1991).

11. A. P. Malshe, S. M. Chaudhari, S. M. Kanetkar, S. B. Ogale, S. V. Rajarshi, and S. T. Kshirsagar, J. Mat. Res. **4**, 1238 (1989).

12. S. Fujimori, T. Kasai, and T. Inamura, Thin Solid Films **92**, 71 (1982).

13. J. J. Cuomo, D. L. Pappas, J. Bruley, J. P. Doyle, and K. L. Saenger, J. Appl. Phys. **70**, 1706 (1991).

14. L. C. Feldman and J. W. Mayer, *Fundamentals of Surface and Thin Films Analysis*, (North-Holland, New York, 1986), p.59. FRD

15. David, F. Edwards and H. R. Philipp, *Handbook of Optical Constants of Solids*, ed. E. D. Palik, (Academic Press, San Diago, 1985) p. 665.

16. A. Borghesi and G. Guizzetti, *Handbook of Optical Constants of Solids II*, ed. E. D. Palik, (Academic Press, Inc., San Diago, 1991) p. 449.

17. N. Savvides, J. Appl. Phys. **59**, 4133 (1986).

18. J. Tauc, R. Grigorovici, and A. Vancu, Phys. Status Solidi **15**, 627 (1966).

19. S. D. Berger, D. R. McKenzie, and P. J. Martin, Phil. Mag. Lett. 57, 285 (1988).

20. J. J. Cuomo, J. P. Doyle, J. Bruley, and J. C. Liu, J. Vac. Sci. Technol., 9, 2210 (1991).

21. R. M. Silverstain, G. C. Bassler, and T. C. Morrill, "Spectrometric Identification of Organic Compounds", 5th ed. (John Wiley and Sons, New York, 1991) p.91.

22. D. Lin-Vien, N. B. Colthup, W. G. Fateley, and J. G. Grasselli, *The Handbook of Infrared and Raman Characteristic Frequencies of Organic Molecules*, (Academic Press, New York, 1991).

23. D. S. Knight and W. B. White, J. Mat. Res. 4, 385 (1989).

24. F. Tuinstra and J. L. Koening, J. Chem. Phys. 53, 1126 (1970).

25. S. K. Hark, M. A. Machonkin, F. Lansen, M. L. Slade, and B. A. Weinstein, AIP Conf. Proc. 120, 465 (1984).

26. F. W. Smith, J. Appl. Phys. 55, 764 (1984).

27. G. K. Hubler, MRS Bulletin 17, 26 (1992); and review articals therein.

28. J. T. Cheung and H. Sankur, CRC Crit. Rev. Solid State Mat. Sci. 15, 63 (1988).

29. G. Koren, A. Gupta, R. I. Baseman, M. I. Lutwyche, and R. B. Laibowitz, App. Phy. Lett. 55, 2450 (1989).

30. G. L. Doll, J. A. Sell, L. Salamanca-Riba, and A. K. Ballal, Mat. Res. Soc. Symp. Proc. Vol. 191, 55 (1990).

31. P. T. Murray, and D. V. Dempsey, Mat. Res. Soc. 1991 Fall Meeting Presentation Abstract, B9.3/A16.3.

32. D. Thebert-Peeler, P. T . Murray, L. Petry, and T. W. Haas, Mat. Res. Soc. Symp. Proc. (Fall 1991) (to be published).

FIGURE CAPTIONS

Figure 1. Schematics of the experimental setup for pulsed laser deposition of thin films.

Figure 2. The spectrum (o) of high energy ion forward recoil scattering from a pulsed-laser-deposited DLC film on Si(100) substrate to show hydrogen content in the film. A spectrum (+) taken from hydrogen implanted amorphous Si (H_{2+} at 25 keV 1×10^{17} ions/cm^2) is shown for a comparison.

Figure 3. Hardness (o) and elastic modules ($\triangle$) of a pulsed laser deposited DLC film (140 nm thick) on Si(100) substrate measured by nanoindentation at three penetration depths.

Figure 4. Real part (n) and imaginary part (k) of the complex refractive index of ArF pulsed laser deposited DLC films on Si(100), reduced from the spectroscopic ellipsometry measurement. The n values for diamond (from Ref. 15) and graphite (from Ref. 16) are also plotted for comparison.

Figure 5. Plot of the quantity $E\varepsilon_i^{1/2}$ versus the photon energy, E, from the data shown in Figure 4. The tangential extrepolation gives the optical band gap of the amorphous material.
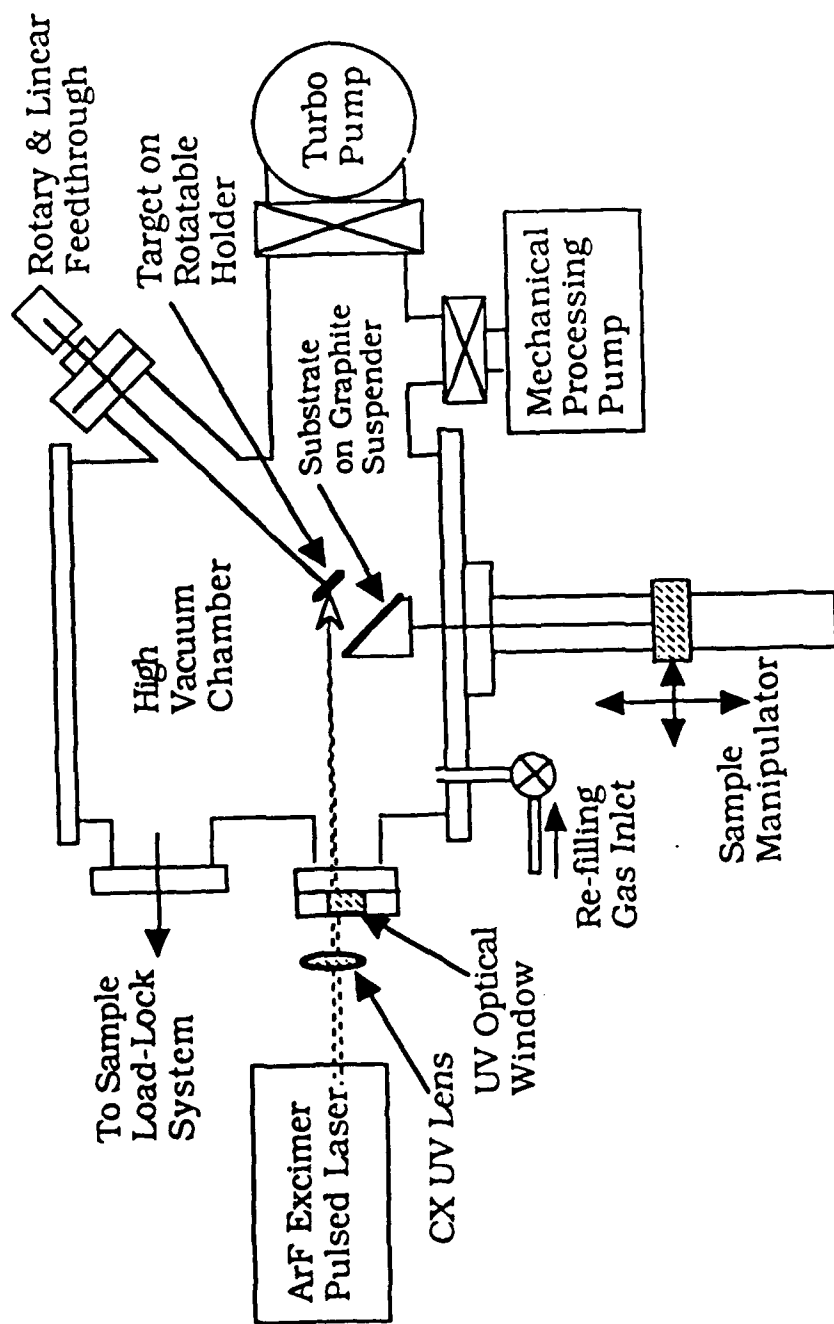
Figure 6. Spectra of electron energy loss spectroscopy of ArF pulsed laser deposited DLC films on Si(100) and NaCl substrates, a) the low loss region and b) carbon K-edge core loss region. Spectra of polycrystalline CVD diamond and pyrolytic graphite taken at identical condition are also shown for comparison.

Figure 7. Raman spectrum of an ArF pulsed laser deposited DLC film on Si(100). Raman spectrum of a pyrolytic graphite target is also shown for comparison.

16

Figure 8. Plot of the quantity $E\varepsilon_i^{1/2}$ versus the photon energy, E, for ArF pulsed laser deposited DLC films deposited at room temperature and subsequently annealed at 300, 450, 600, and 800 °C in a vacuum. The tangential extrapolation gives the optical band gap (E_g), of the amorphous films.

Table 1. Summary of results of a-C films deposited by laser ablation

Deposition Conditions	Results	References
CW CO_2, 5×10^8 W/cm^2	conductive, opaque, soft	12
Pulsed Ruby (694nm) 6.7×10^8 W/cm^2	insulation $Eg=1.25$ eV	11
Nd:YAG (1064 nm) $>5 \times 10^{10}$ W/cm^2	hard, 8 Moh's scale $Eg=0.4$ eV	8
Nd:YAG (532nm) 5×10^{11} W/cm^2 plus a high current discharge	$HV=13\text{-}37$ GPa. $Eg=1.0$ eV, 75% sp^3	9-10
XeCl (308nm), 3×10^8 W/cm^2	hard, $Eg=1.4$eV (H/C=0.3)	7
XeCl (308nm), 1.25×10^8 W/cm^2 plus a capacitor discharge	$HV=19\text{-}27$ GPa $Eg=1.27$ eV	6
KrF (248 nm) $\sim 10^9$ W/cm^2	26 GPa, DLC	5
KrF (248 nm) 1.4×10^8 W/cm^2	$Eg=1.7$ eV, 85% sp^3	4
ArF (193nm), 5×10^8 W/cm^2	$HV=30\text{-}38$ GPa $Eg=2.6$ eV, 95% sp^3	This work

Rotary & Linear Feedthrough

Target on Rotatable Holder

Turbo Pump

Substrate on Graphite Suspender

Mechanical Processing Pump

High Vacuum Chamber

To Sample Load-Lock System

Re-filling Gas Inlet

Sample Manipulator

ArF Excimer Pulsed Laser

CX UV Lens

UV Optical Window

Pulsed Excimer Laser Ablation System for Film Deposition

Fig. 1

Fig 22

Fig 3
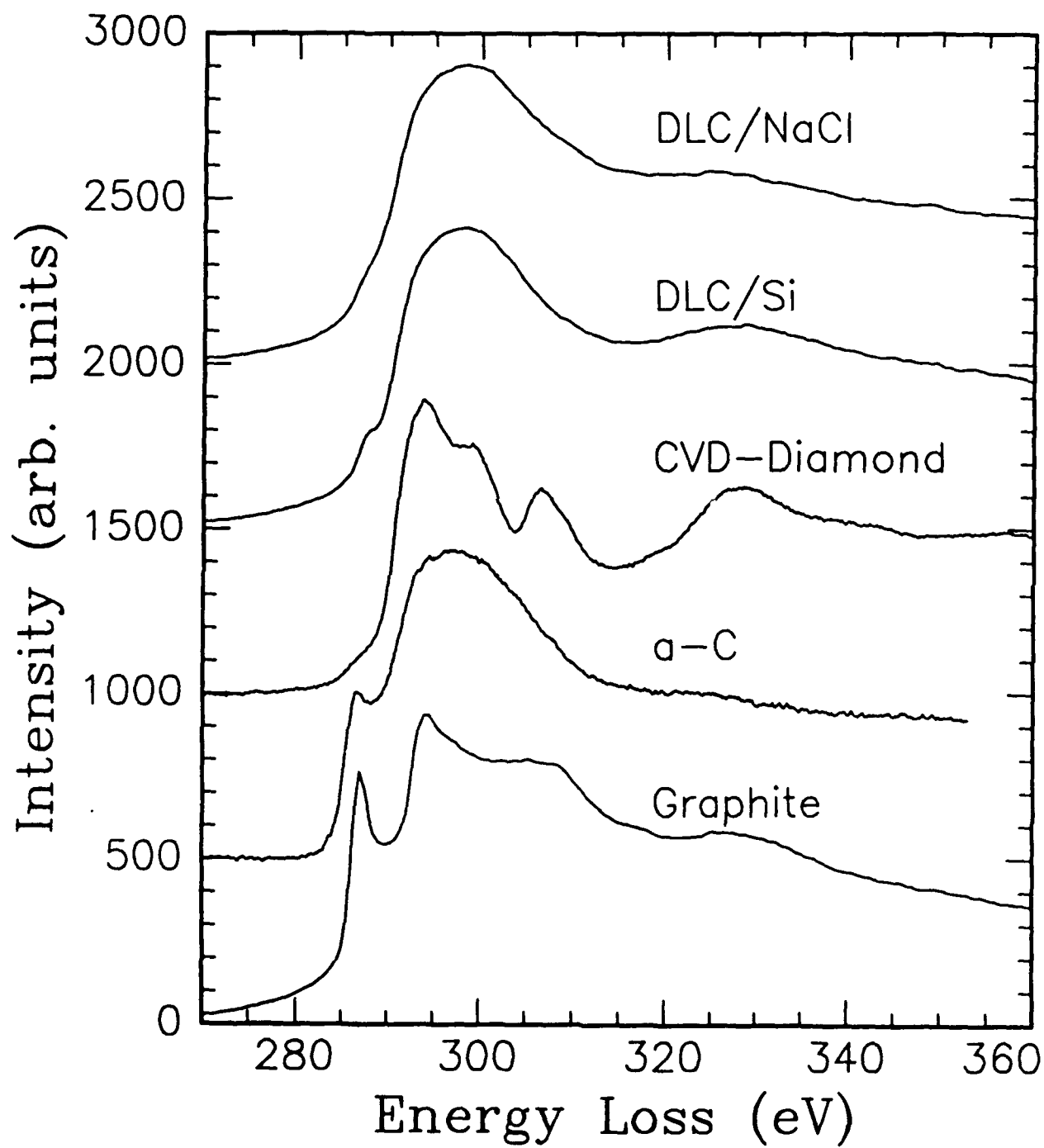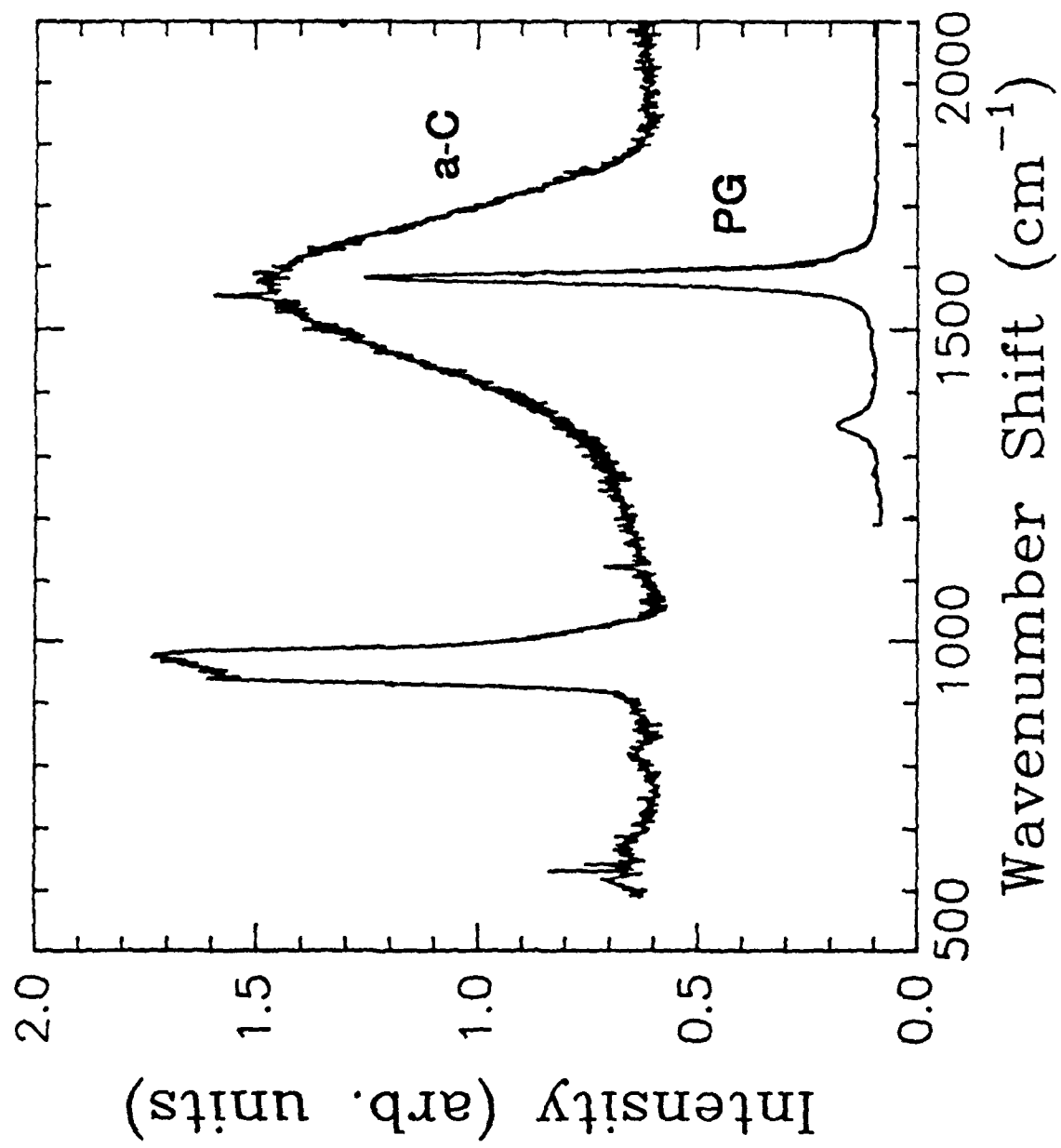
Photon Energy (eV)

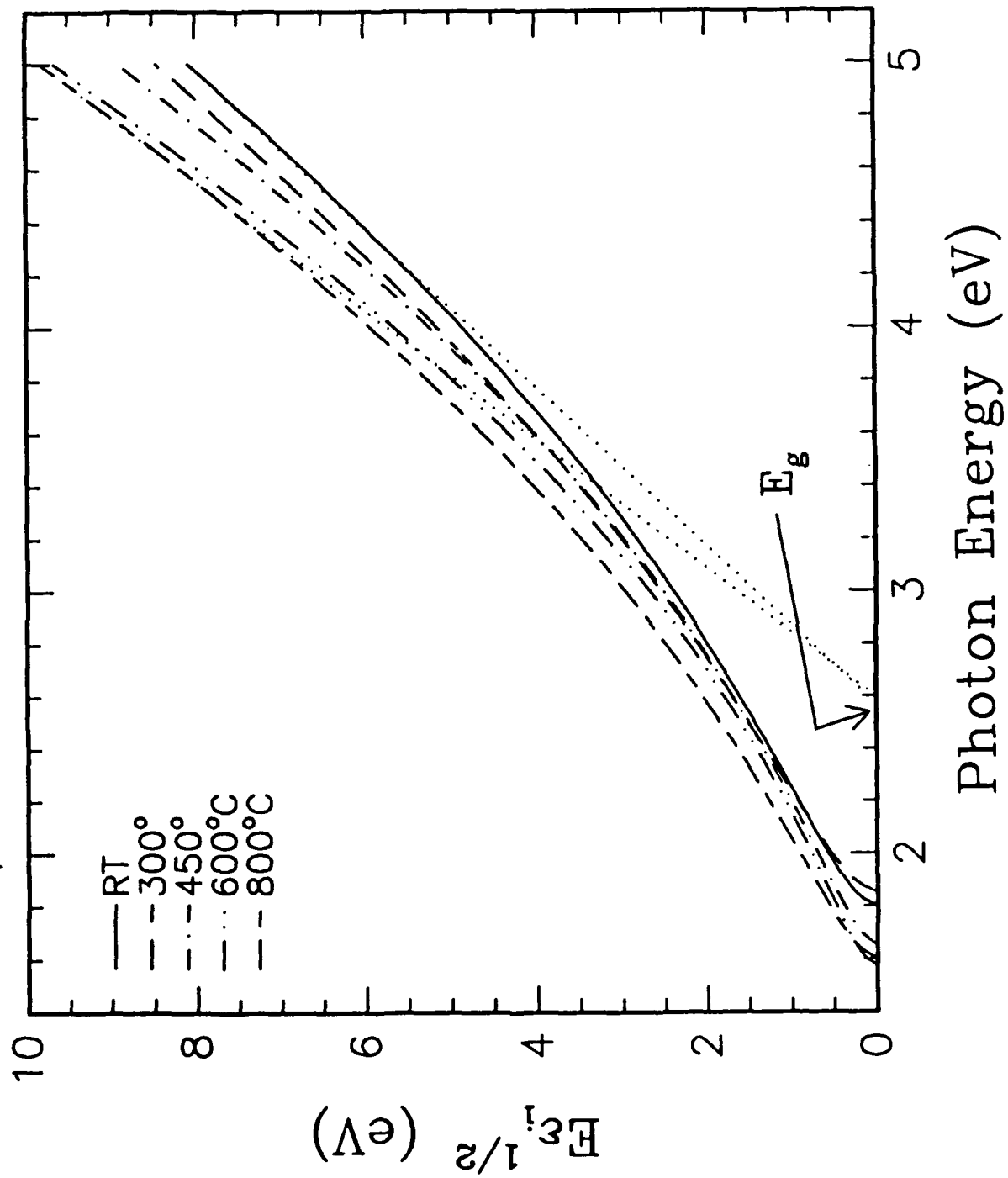$E\varepsilon_i^{1/2}$ (eV)

E_g
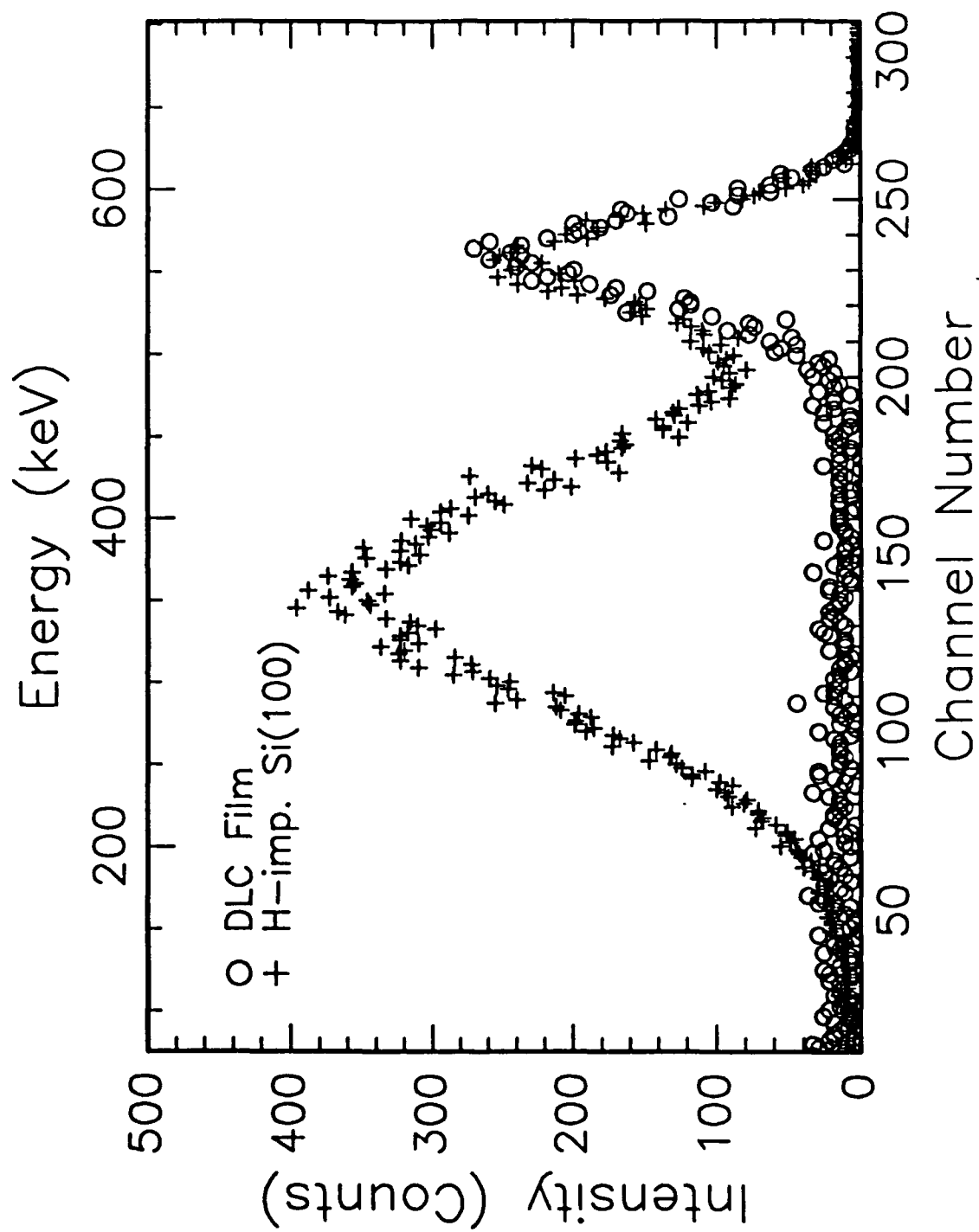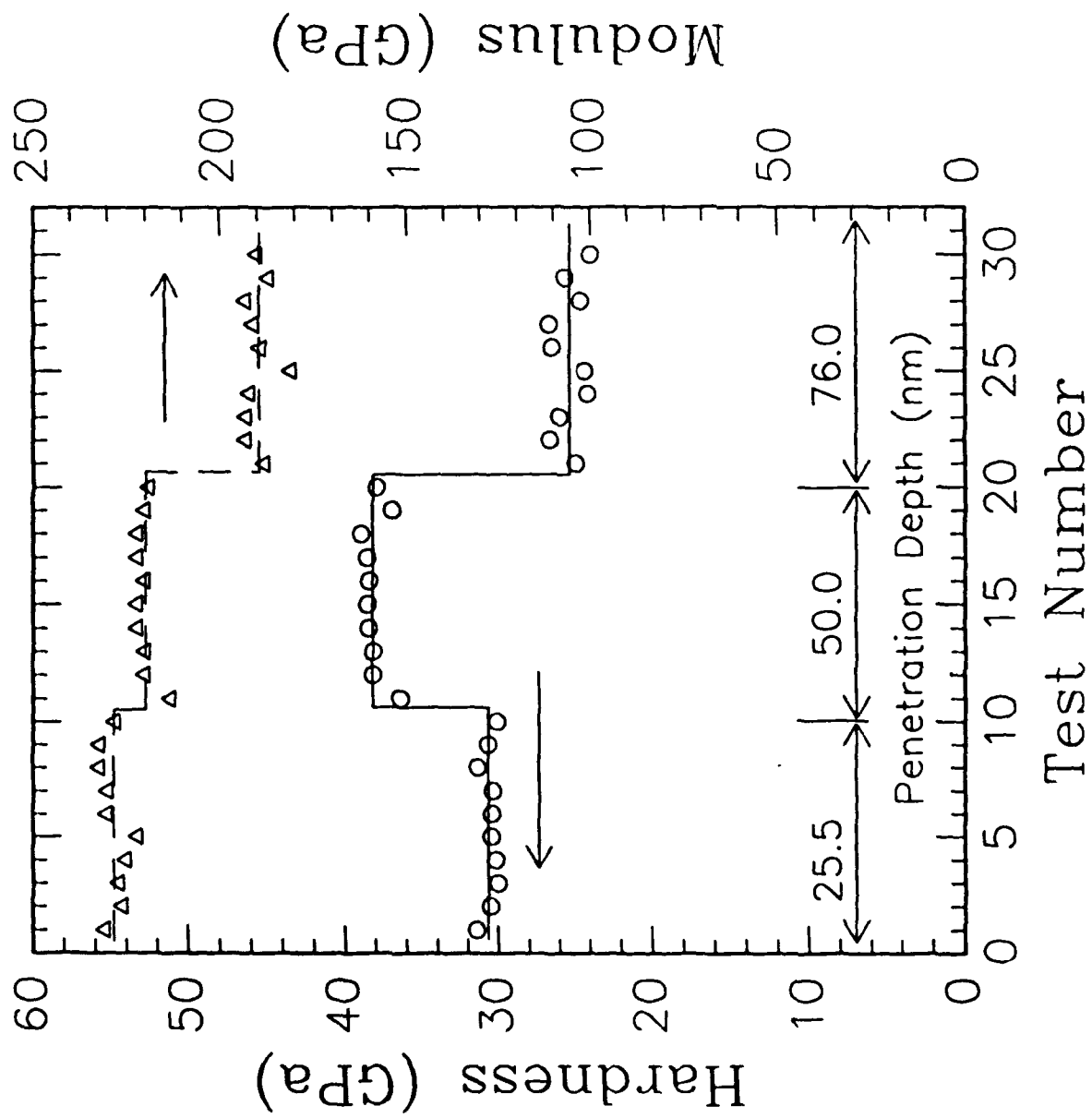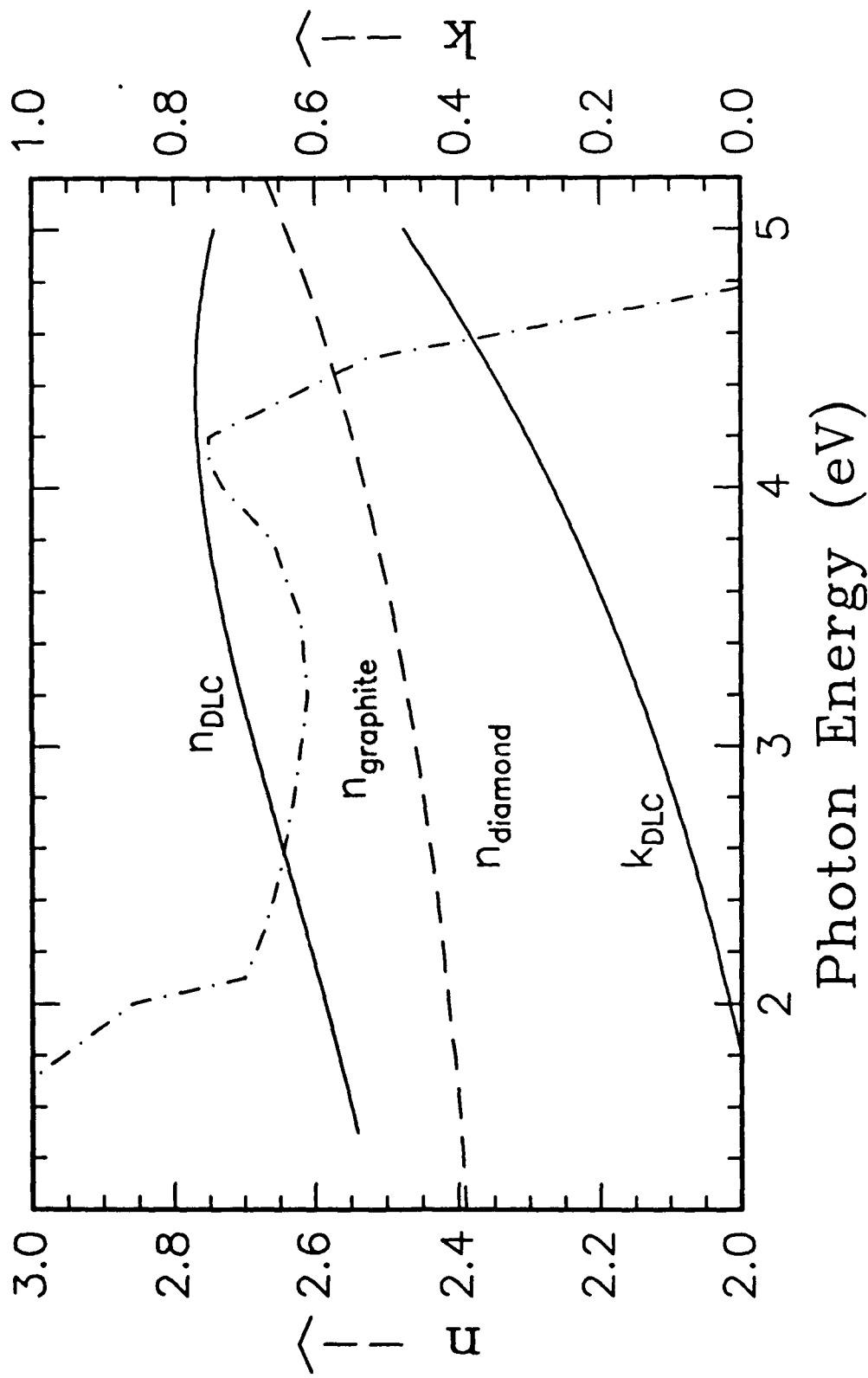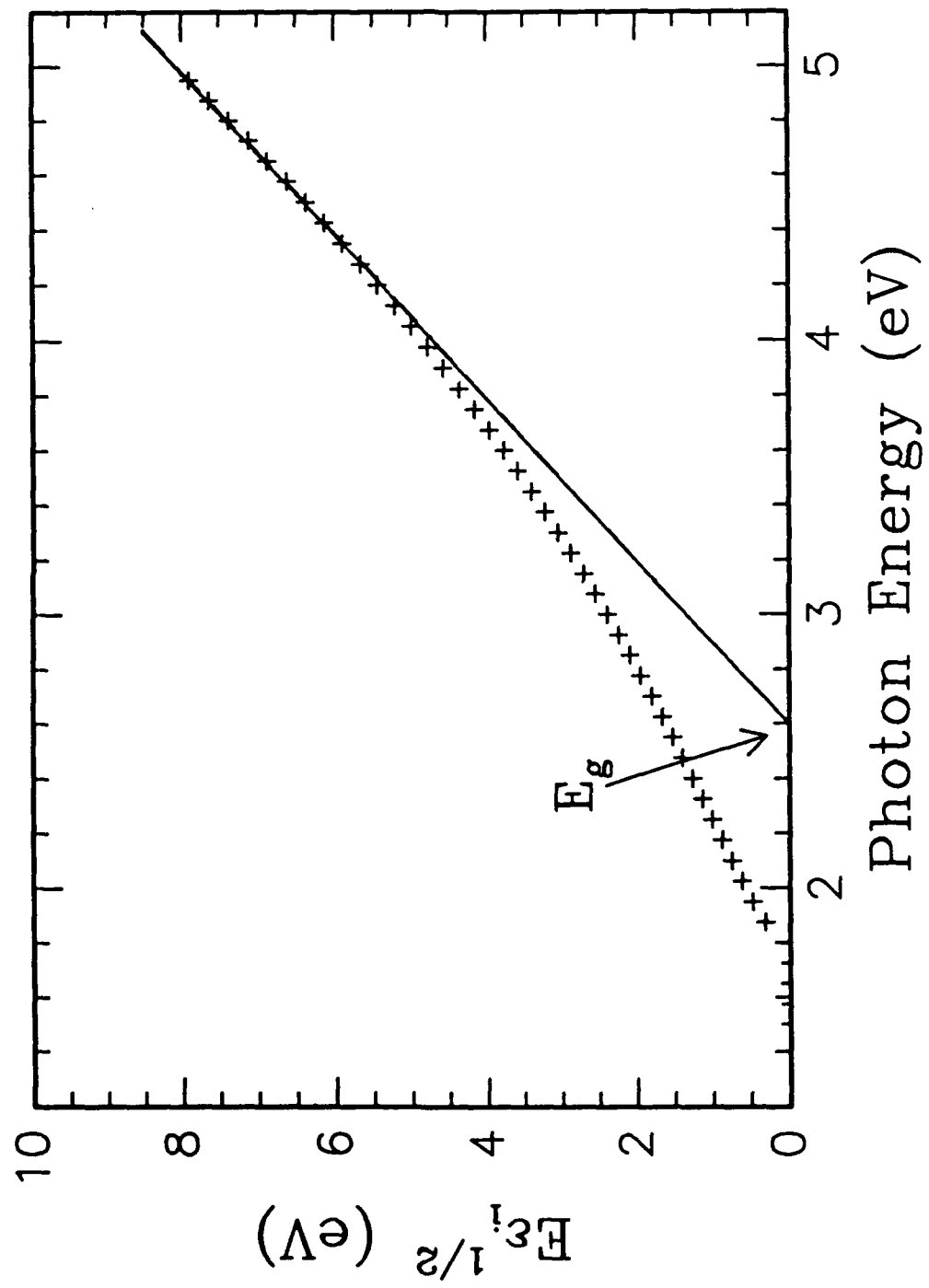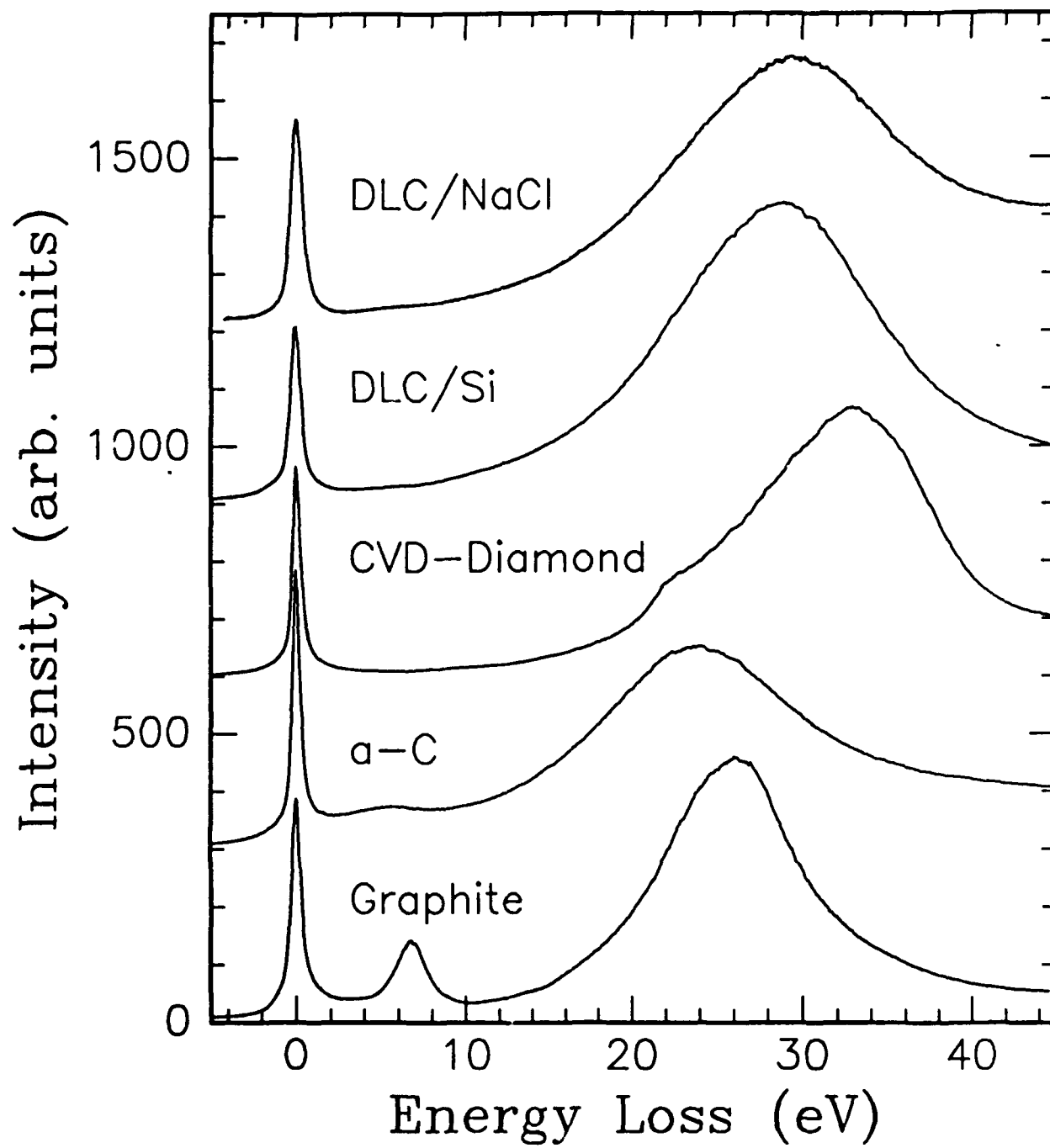
TECHNICAL REPORT DISTRIBUTION LIST - GENERAL

Office of Naval Research (2)*
Chemistry Division, Code 1113
800 North Quincy Street
Arlington, Virginia 22217-5000

Dr. James S. Murday (1)
Chemistry Division, Code 6100
Naval Research Laboratory
Washington, D.C. 20375-5000

Dr. Robert Green, Director (1)
Chemistry Division, Code 385
Naval Air Weapons Center
  Weapons Division
China Lake, CA 93555-6001

Dr. Elek Lindner (1)
Naval Command, Control and Ocean
  Surveillance Center
RDT&E Division
San Diego, CA 92152-5000

Dr. Bernard E. Douda (1)
Crane Division
Naval Surface Warfare Center
Crane, Indiana 47522-5000

Dr. Richard W. Drisko (1)
Naval Civil Engineering
  Laboratory
Code L52
Port Hueneme, CA 93043

Dr. Harold H. Singerman (1)
Naval Surface Warfare Center
  Carderock Division Detachment
Annapolis, MD 21402-1198

Dr. Eugene C. Fischer (1)
Code 2840
Naval Surface Warfare Center
  Carderock Division Detachment
Annapolis, MD 21402-1198

Defense Technical Information
  Center (2)
Building 5, Cameron Station
Alexandria, VA 22314

* Number of copies to forward